Materials Research Express

PAPER

Resistivity humidity sensors based on hydrogenated amorphous carbon films

Materials Research Express

PAPER

Resistivity humidity sensors based on hydrogenated amorphous carbon films

RECEIVED
6 September 2018

REVISED
18 October 2018

ACCEPTED FOR PUBLICATION
1 November 2018

PUBLISHED
14 November 2018

Javier Epeloa[1], Carlos E Repetto[1], Bernardo J Gómez[1], Lucas Nachez[2] and Ariel Dobry[1]

[1] Facultad de Ciencias Exactas Ingeniería y Agrimensura, Universidad Nacional de Rosario and Instituto de Física Rosario, Bv. 27 de Febrero 210 bis, S2000EZP Rosario, Argentina
[2] INFES/IF Universidad Federal Fluminense, 28470-000, Santo Antônio de Pádua, Brazil

E-mail: bgomez@ifir-conicet.gov.ar

Keywords: amorphous carbon films, humidity Sensors, impedance spectroscopy

Abstract

We have studied the humidity dependence of the electrical properties in hydrogenated amorphous carbon (a-C:H) films. The films were prepared in two stages combining the techniques of physical deposition in vapor phase evaporation (PAVD) and plasma pulsed nitriding. They were deposited over printed circuit boards made of synthetic resin FR2, predesigned to measure DC and AC transport. The Raman spectrum showed a broad peak whose two components are characteristics of a-C:H. By treating the sample in N_2-H_2 plasma, the impedance became intrinsically sensitive to the relative humidity (RH) of the surrounding media. We observed that when RH increased, the electrical impedance (Z) of the films diminished. The complex impedance spectroscopy method was used to analyze the interaction between the water molecules and the a-C:H film. The main contribution to the humidity dependency of Z came from the resistivity component. The present work provides a fundamental support to develop humidity sensors based on the variation of the impedance of a-C:H films.

1. Introduction

Humidity sensors are widely used in food quality monitoring, meteorology, medical equipment, and so forth. The research to develop new materials for smaller and cheaper humidity sensors has attracted increasing interest [1]. For example, in the measurements of altitude dependence of the vapor profile of the atmosphere, using radio-sounding systems [2], ultrafast humidity sensors are necessary. A recent new application of ultrafast sensors was proposed for a touch-less user interface proving to run in a whistling recognition analysis [3].

With the exfoliation of graphene in 2003, a new route for carbon based electronic devices has been opened [4]. Functionalized graphene constitutes a set of two dimensional material whose electronic properties are highly dependent on different molecules present in the near environment. Therefore, they are promising materials for biological and chemical sensors [5]. In particular, the electrical resistance of graphene oxide (GO), which can be viewed as an oxidation product of graphene, has been shown to be humidity dependent [6]. Moreover, in a recent work, it has been shown that even a single-layer chemical vapor deposited (CVD) graphene has humidity sensitivity as seen from the variation of its resistance [7].

Otherwise amorphous carbon films were discovered some time ago [8]. They are noncrystalline disordered structures having any mixture of sp^3, sp^2, and even sp^1 hybridization. It is also possible the presence of hydrogen bond, giving rise to the hydrogenated amorphous carbon (a-C:H). Films of a-C:H were originally developed for protective coating. The use of these films in electronic devices has been evaluated during the last years. For example, the potential application in field emission microelectronic devices has attracted great attention [9]. Furthermore, capacitive humidity sensors based on a-C:H deposited on n-Si have been recently proposed [10].

In this paper we are reconsidering a-C:H to be used as humidity sensors. We start by generating a-C:H from graphite rods in a PAVD [11]. The resulting films are modified by N_2-H_2 plasma treatment. The micro-structure was characterized by the Raman scattering. Then, it was obtained the complex impedance as a function of the

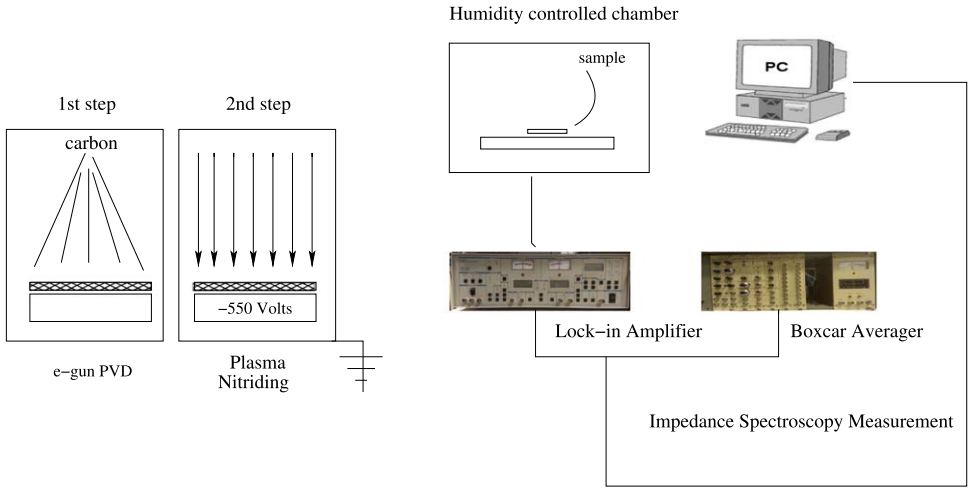

Figure 1. Left: scheme of the two step synthesis process. First, the carbon evaporated from a graphite rod is deposited on a substrate. Second, the film is exposed to a H_2-N_2 plasma. Right: diagram of the humidity chamber and the impedance measurement equipment.

relative humidity (RH). Finally, we show that the capacity only changes if RH is high enough, this is different from what was found in [10] for a-C:H/n-Si heterojunctions. However, the resistance has a strong variation in a wider humidity range. In fact, the relative sensitivity of the resistance versus humidity is greater than the one obtained for the capacitance at low frequency in figure 3 of [10]. This suggests that films of modified a-C:H could be the basis of resistance humidity sensors.

2. Synthesis of a-C:H films by an e-beam evaporator

Figure 1 shows a picture of the deposition system. A stainless steel chamber was evacuated to about 10^{-6} Torr by an oil diffusion pump with a liquid nitrogen trap. The graphite rods were irradiated with an electron-beam, with the aim of producing carbon films. The irradiation of the samples was performed using an electron beam accelerator, whose energy and current are of approximately 4000eV and 200 mA, respectively. Considering the operating conditions of the device, we can assure that we are working in a regime without collisions, i.e. in a ballistic regime for the evaporated carbon atoms.

Later, the sample was placed in a plasma nitriding reactor originally designed to treat the surface of the steels. The purpose of this procedure was to dilute the sample to increase the resistance and to change the microstructure of the surface by interaction with the plasma.

Through this treatment, the samples showed sensitivity to humidity, as we will see in the next sections.

The reactor consists of an 8-litre AISI 304 stainless steel vacuum chamber connected to ground potential. Inside the chamber, there is an electrode, also made of AISI 304 stainless steel, connected to a power supply that can generate a square-wave signal of up to 700 V at a frequency between 0 and 1 kHz. The duty cycle can also be changed. A pre-vacuum of 0.001 Torr was created in the chamber, which was then back filled to 1 Torr with a mixture of 50% nitrogen and 50% hydrogen. We conducted our experiments at a constant temperature of 250°C, with an on/off ratio of 50%/50% at a frequency of 100 Hz. The applied voltage was 550 V. Pressure, current, voltage and flux were kept constant during the ion nitriding treatments. The treatments lasted 20 min; measured from the moment the sample temperature reached 50°C.

3. Raman characterization

Raman spectra were obtained with a Witec Alpha 300 SR Confocal Raman Microscope equipped with a CCD detector, cooled by a Peltier cell, and a solid-state Nd:YAG laser of 532 nm wavelength. The optical microscope was operated with a 20× lens and a diffraction grating of 600 lines/mm. A region of the characteristic spectrum of a Diamond-like carbon structure can be observed in figure 2, once the luminescent background was subtracted. Two main bands, corresponding to the D and G modes, can be observed. The G mode refers to the bond stretching of pairs of sp^2 carbon atoms at 1563 cm^{-1}, and the D mode refers to the breathing of the aromatic rings [12, 13] at 1409 cm^{-1}. The Raman spectra seen in figure 2 is characteristic of a-C:H as it is shown in [13] and [14].

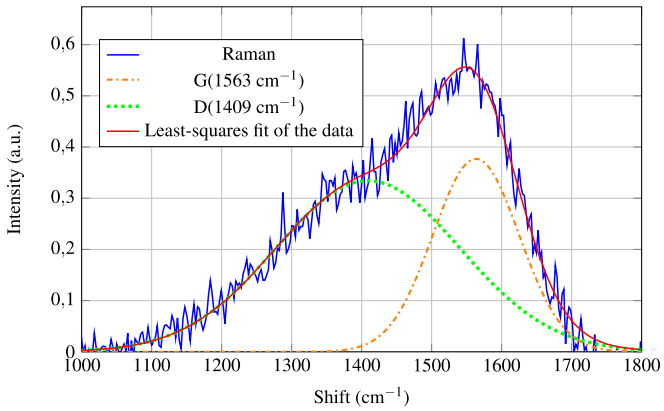

Figure 2. The Raman spectra in the relevant energy zone. We show a deconvolution on two Gaussian peaks corresponding to D and G modes (see text).

It is worth discussing the microstructure of the film in light of a recent Molecular Dynamics (MD) simulation [15]. In this paper it has been shown that the relative density and the sp_3 fraction increase with the energies of the incident hydrocarbon and then they become stabilized. In our case, where carbon atoms are ejected from the target by evaporation, the incident energies are much smaller than those studied in [15]. The structure is not yet stabilized, it could incorporate H_2 or N_2 when it is exposed to the plasma. This could be important for the interaction between the film and water molecules, as we are going to analyze in section 4.3.

4. Results and discussion

4.1. AC complex impedance spectroscopy for various humidity conditions

In this section we are studying the evolution of the complex impedance of the films as RH varies. To this end, we have used a temperature and humidity controlled chamber. We used a reference commercial sensor SHT 71 (www.sensirion.com) to obtain the temperature and the humidity inside of the chamber.

Within the chamber, we disposed a heating resistor, the RH is changed by evaporating a water drop on a heater, using the aforementioned resistor. The variation of the temperature using this method is less than 1 degree Celsius, and it allows a variation of the humidity in the range from 10% to 100%.

To reduce the initial humidity inside the chamber we used dry air (10% of humidity). After the introduction of dry air, the heating resistor is powered on and the water drop is thrown over it. Using this method, the humidity changed but the temperature remained almost constant $(20 \pm 1)^{\circ}$C.

The electrical characterization of the film was performed using a lock-in amplifier SR530 from Stanford Research System. The films were connected to the signal reference of the amplifier (1 V peak to peak) to obtain the current over them. By measuring the current on the films, the complex impedance at different frequencies was obtained.

The lock-in amplifier was connected to the computer using a PC interface SR280 from Stanford Research System. Using Matlab software we processed the data of the complex current measurements of the lock-in amplifier to transform them into a complex impedance. At the same time, we controlled the frequency of the signal lock-in reference, the humidity and temperature inside the chamber. This information was stored in real time into the computer.

First, we set the lock-in signal reference at constant frequency. Then, we changed the condition of RH inside the chamber between 20% and 90% to perform the measurements on the thin film. Thereby, we obtained a family of curves for different values of frequencies. In figure 3 we plot the imaginary part of the complex impedance, $\Im(Z)$, versus the real part of the complex impedance, $\Re(Z)$, for different frequencies of the AC signal (1 kHz, 2.5 kHz, 5 kHz and 20 kHz).

All the curves meet in the region of high RH, which appears in figure 3 at the left bottom corner (the lower values of Z). As f increases, the ranges of variation of both $\Re(Z)$ and $\Im(Z)$ decrease.

This situation can also be seen in figure 4 where the variation of the $|Z|$ due to RH is shown for different values of f. The sensitivity of $|Z|$ to RH depends on the exciting frequency. The lower the frequency, the greater the range of variation of $|Z|$ due to RH. This behavior suggests that the measurements of the low frequency impedance could be used in future devices based on a-C:H films. From the lower frequency ($f = 1$ kHz) dependency of $|Z|$ with RH ranging between 30% and 90%, we can define a sensor sensitivity as $S = \frac{|Z_{30}| - |Z_{90}|}{|Z_{30}|}$ which is 0.99. This value is higher than the one obtained from the low frequency capacity of a-C:H/n-Si

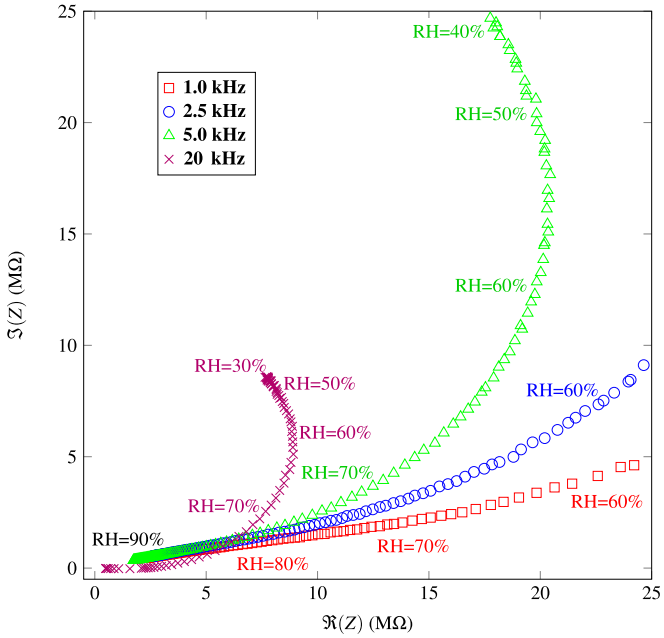

Figure 3. Imaginary part versus real part of the complex impedance for different frequencies, while varying the relative humidity conditions between 30% and 90%.

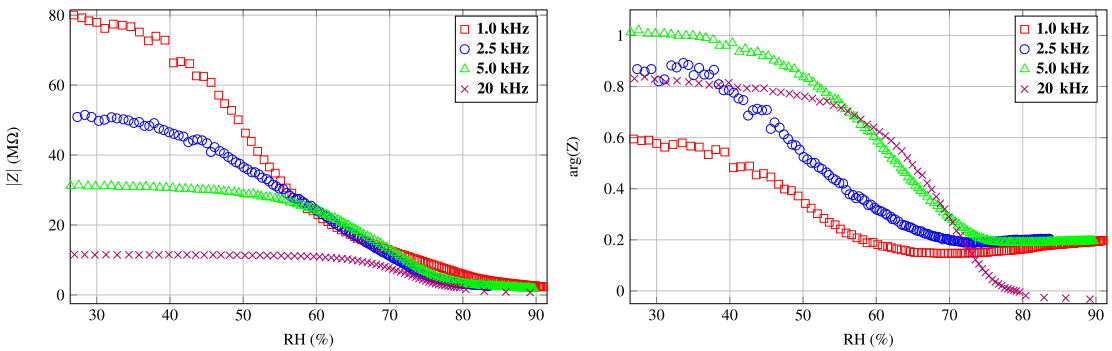

Figure 4. Impedance modulus and phase versus relative humidity, for different frequencies.

heterojunctions [10] ($S = 0.56$ for the same humidity range). It is of the same order of magnitude as the previous analyzed materials like Carbon-Nitride films [16] ($S = 0.94$) and of processable polyaniline blend [17]($S = 0.89$).

We will see that the main dependency of the impedance on the variations of RH comes from the resistivity component of Z. Therefore, the films of a-C:H have better properties sensing humidity when they are used as resistive sensor than if they are used as capacitive sensor. It is worth mentioning that in a recent work, it has been demonstrated that a single layer graphene placed on top of SiO_2 substrate could act as humidity resistivity sensor [7]. Its sensitivity is $S = 0.31$ but it has a broad sensitivity range and fast recovery time.

4.2. Equivalent circuit of the a-C:H film

To discriminate the different contributions to Z and understand the underlying mechanism, we have transformed the RH-dependence of $\Re(Z)$ and $\Im(Z)$ into the f-dependence at different RH. This is the so called Nyquist plot of impedance [18].

Then we adjusted the measured data to an equivalent circuit as shown in figure 5. R and C represent the contribution to resistance and capacitance arising from the a-C:H film as well as the possible contribution of the substrate material. r refers to the contact resistance. The curves of figure 6 represent the least squares adjustment of the data obtained from the real, $\Re(Z)$, and imaginary part, $\Im(Z)$, of the impedance as a function of the frequency, for different RH values. The adjustment function corresponds to the model of the equivalent circuit shown in figure 5:

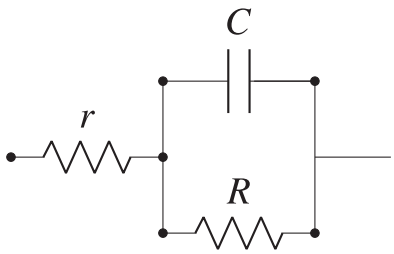

Figure 5. Equivalent circuit used to fit the measured impedance.

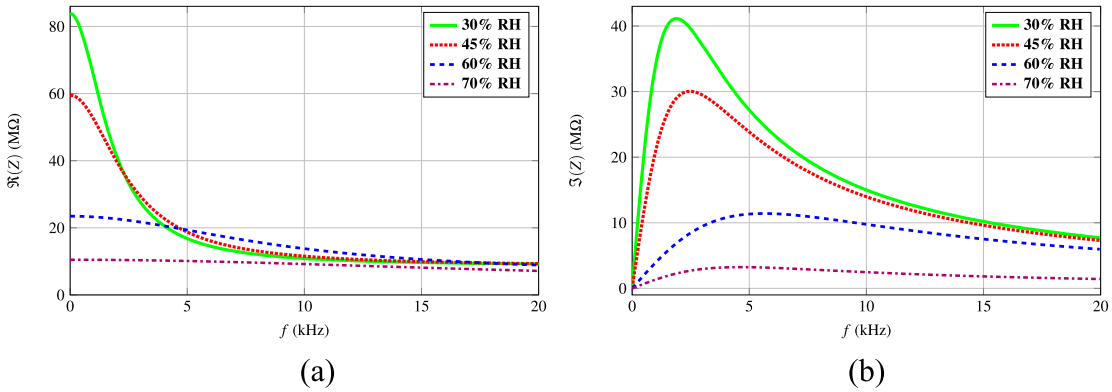

Figure 6. Real (a) and Imaginary (b) part of the complex impedance versus frequency, for different relative humidity conditions.

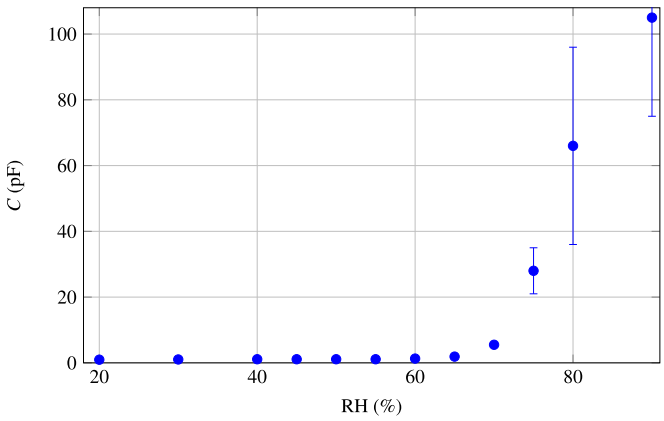

Figure 7. Humidity dependency of the capacity.

$$\Re(Z) = r + \frac{R}{1 + (\omega CR)^2},$$
$$\Im(Z) = \frac{R^2 C\omega}{1 + (\omega CR)^2}, \quad (1)$$

where $\omega = 2\pi f$. For each of these curves, i.e. for each value of RH, corresponding values of C and R are obtained. The dependence of R and C due to the different value of RH can be observed in figures 7 and 8.

From figure 7, it can be seen that the capacity C is kept constant for values of RH lower than 60%, and above this RH value C grows up to two orders of magnitude.

The humidity dependency of the capacity was previously studied in a-C:H films deposited on n-silicon [10]. The authors relate the variation of the capacity due to the humidity with the increase in the amount of physisorbed water having a dipole moment. However, we cannot assert that the same mechanism works in our case. On one hand, the capacity depends on RH only above 60% and does not depend on the frequency. On the other hand, the resistance depends on the humidity for all values of RH as can be seen in figure 8. At RH $<$ 40%

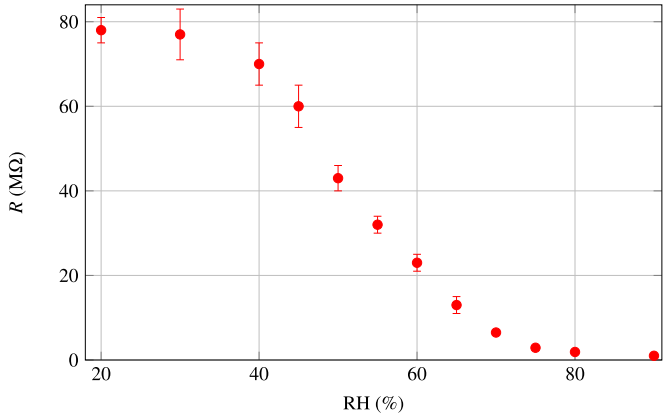

Figure 8. Humidity dependency of the resistance.

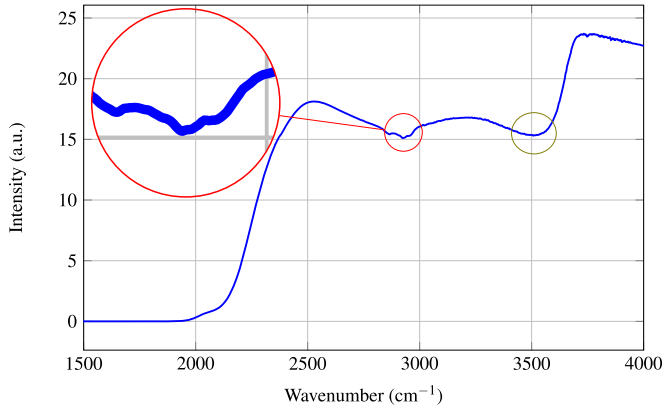

Figure 9. IR spectrum of the film studied. The characteristic sector that shows the presence of C–H bonds is shown in the zoom area. In the circle on the right, a region of the spectrum corresponding to hydroxyl groups is identified.

the dependency is weaker. When RH increases, a crossover takes place. R falls sharply for RH $>$ 40%. Finally, when the humidity is high enough (RH $>$ 80%), the surface is saturated and R does not depend essentially on RH.

4.3. Possible interaction mechanism between the film and water molecules

Let us analyze the possible microscopic process involved in the change of the electrical conduction as RH increases. This process should be analogous to that suggested for GO films to explain the humidity sensitivity [6]. Probably, at lower RH, chemisorption is the dominant effect where the water molecules combine at the surface with the N_2 or H_2 molecules inserted in the a-C:H films to form hydroxyl. The mobility of hydroxyl ions can occur via a proton transfer mechanism as discussed in [1].

By increasing RH, the protons (H^+) arising from hydroxyl attached to the surface are bonded to the excess adsorbed water molecules to form hydronium (H_3O^+) ions. An ionic layer forms on the surface, giving an additional mechanism for the electrical conduction. The density of the hydronium ions increases with RH. This mechanism could, in principle, explain the rapid decrease of R for high enough RH.

To clarify the previous assumption, we have characterized the film by IR spectroscopy using the Spectrometer One by Perkin-Elmer. The results obtained are shown in figure 9, the characteristic response due to the presence of C-H bonds [19] and hydroxyl groups [20] in the film was observed. This reinforces our proposed mechanism.

Besides, the similarity with GO films appears clearly if we observe that the dependence of R on RH can be approximated by an exponential relationship, which we express as follows

$$\log(R/R_0) = \beta \times (\mathrm{RH}-\mathrm{RH}_0) + h, \tag{2}$$

where R_0 is a reference resistance at RH $=$ RH$_0$.

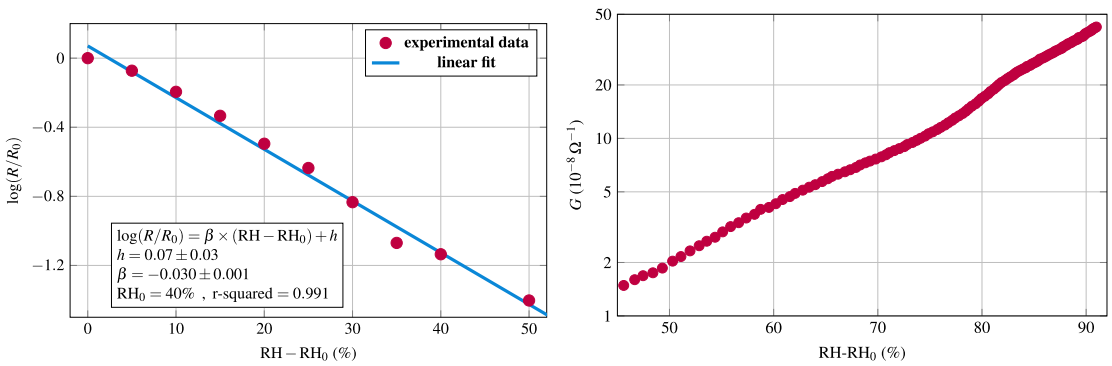

Figure 10. (left) Fitting of the experimental data of resistance versus RH by using the equation (2). (right) Measured conductance of the film at 1 kHz.

In figure 10, the graphic on the left shows the values of $\log(R/R_0)$ versus HR-HR$_0$. The data of the measurements follows a linear behavior, so they can be fitted by means of equation (2) and the fitting parameters are shown in the inset of that figure.

This exponential behavior with RH is also observed when measuring the conductance G of the film. This is shown in figure 10, in the graphic on the right. A similar logarithmic fitting was found in GO samples as a function of the RH and the temperature [3].

Moreover, we have checked that the sample remains humidity sensitive for at least nine month. It is worth mentioning that the sample, during this period, was subjected to a large number of cycles of changes in the condition of relative humidity, as well as to the study and characterization of its electrical properties by impedance spectroscopy.

Finally, we have not observed appreciable signs of hysteresis in the behavior of the impedance when raising or lowering the humidity.

5. Conclusions

In summary a-C:H films were deposited over printed circuit boards made of synthetic resin FR2 with copper terminals designed for the electrical characterization and then they were treated by N_2-H_2 plasma. After this treatment, the AC response of the films was obtained by a lock-in amplifier, using a temperature and humidity controlled chamber. Our results show that the impedance of the films depends on the relative humidity. We assume that the treatment processing changed the micro-structure in a way that the electrical transport properties of the films became humidity dependent. This effect could be similar to the one observed in GO.

Besides, we have analyzed the experimental data by means of an equivalent circuit. This analysis showed that the resistivity component of the impedance is the main responsible for the humidity sensitivity of the film.

Specifically, the dependency of the impedance on the humidity can be used to design future nanoscopic sensors based on a-C:H films.

Acknowledgments

We acknowledge O Fojón, and G Lacconi for their useful discussion and critical reading of the manuscript. We acknowledge G Baranello, H Rindizbacher and Javier Cruceño for their essential contributions to resolving all the technical issues to undertake the present work. This work was supported by PICT-2013-0544 of the ANPCyT.

ORCID iDs

Bernardo J Gómez https://orcid.org/0000-0002-9573-2911

References

[1] Farahani H, Wagiran R and Hamidon M N 2014 *Sensors* **14** 7881–939
[2] Ha J, Park K D, Kim K and Kim Y H 2010 *Asia-Pacific Journal of Atmospheric Sciences* **46** 233–41
[3] Borini S, White R, Wei D, Astley M, Haque S, Spigone E, Harris N, Kivioja J and Ryhanen T 2013 *ACS nano* **7** 11166–73

[4] Moldovan O, Iñiguez B, Deen M J and Marsal L F 2015 *IET Circuits, Devices & Systems* **9** 446–53
[5] Liu Y, Dong X and Chen P 2012 *Chem. Soc. Rev.* **41** 2283–307
[6] Yao Y, Chen X, Zhu J, Zeng B, Wu Z and Xiaoyu Li X 2012 *Nanoscale Research Letters* **7** 1–7
[7] Smith A D *et al* 2015 *Nanoscale* **7** 19099–109
[8] Bewilogua K and Hofmann D 2014 *Surf. Coat. Technol.* **242** 214–25
[9] Forrest R, Burden A, Silva S, Cheah L and Shi X 1998 *Appl. Phys. Lett.* **73** 3784–6
[10] Chen H J, Xue Q Z, Ma M and Zhou X Y 2010 *Sensors Actuators* B **150** 487–9
[11] Harsha K S 2005 *Principles of Vapor Deposition of Thin Films* (Amsterdam: Elsevier)
[12] Ferrari A C and Robertson J 2000 *Phys. Rev.* B **61** 14095
[13] Ferrari A C and Robertson J 2004 *Philosophical Transactions of the Royal Society A* **362** 2477–512
[14] Casiraghi C, Ferrari A and Robertson J 2005 *Phys. Rev.* B **72** 085401
[15] Chen Y N, Ma T B, Zhu P Z, Yue D C, Hu Y Z, Chen Z and Wang H 2014 *Surf. Coat. Technol.* **258** 901–7
[16] Lee J G and Lee S P 2006 *Sensors Actuators* B **117** 437–41
[17] McGovern S T, Spinks G M and Wallace G G 2005 *Sensors Actuators* B **107** 657–65
[18] Barsoukov E and Macdonald J R 2005 *mpedance Spectroscopy: Theory, Experiment, and Applications* (Hoboken, NJ: Wiley)
[19] Veres M, Koos M and Pocsik I 2002 *Diam. Relat. Mater.* **11** 1110–4
[20] Socrates G 2004 *Infrared and Raman Characteristic Group Frequencies: Tables and Charts* (New York: Wiley)